

# MODEL SIMPLIFICATION OF LITHIUM-ION BATTERY MODULE HEATING FOR ELECTRIC CARS

<sup>1</sup>CHENG-RONG HUANG, <sup>2</sup>JIK CHANG LEONG

<sup>1,2</sup>Department of Vehicle Engineering NPUST Taiwan  
E-mail: <sup>1</sup>m10338011@mail.npust.edu.tw, <sup>2</sup>jclcong@mail.npust.edu.tw

---

**Abstract-** This paper aims to numerically examine the feasibility of simplifying the heating mechanism of a lithium-ion battery module using the lumped-system approach. Through this approach, the battery module is treated as a rectangular module that produces almost the same amount of heat compared to the battery module that contains 180 IHR 18650 battery cells, which generate heat individually. The mathematical model satisfies conservation laws of mass, momentum, and energy. The results show that by setting the appropriate heat generation rate for the rectangular module, it is absolutely possible for the lumped system model to produce similar temperature fields and heat fluxes without introducing too much discrepancy.

---

**Keywords-** Electric Cars, Lithium-Ion Battery, Temperature, Lumped-System Approach, Discharge Current.

---

## I. INTRODUCTION

The use of gasoline powered cars has, as a result of global warming and serious energy problems, faced enormous challenges. Hence, most major car companies around the world have actively engaged in the development of energy-saving cars, the electric cars in particular. A proper operation of the electrical vehicles requires batteries that are capable of producing high specific power and high specific energy density, but at the same time contributing unsubstancial additional weight to the car. Although lead-acid batteries have long been used in many applications, they are found to be less suitable for electric vehicles when compared to nickel-metal hydride (NiMH) and lithium-ion batteries. As a matter of fact, the energy density associated to lithium-ion batteries is at least four times higher than that of a lead-acid battery, ensuring longer travel distance per charge, sufficient acceleration and greater longevity [1]. Although NiMH batteries are currently the best choice for hybrid electric vehicle battery, their energy density is merely half of the lithium-ion battery. Aside from the thermal safety issue associated to the lithium-ion batteries, they are evidently more compact, lighter in weight, and relatively easier for packaging [2]. Once the thermal safety issue is addressed, lithium-ion battery will surely win the competition for future applications in electric vehicle.

To be used in any electric vehicle, a number of lithium-ion cells are inter-connected either in series or in parallel with each other to form battery modules, that are then inter-connected to form a batter pack. Lithium-ion batteries are generally well recognized for their high voltage, high specific energy, high specific power, long life, and low self-discharge characteristic. In contrast to valve-regulated lead-acid or NiMH batteries, lithium-ion batteries are always criticized for their higher volumetric heat generation rate [2]. Hence, effective schemes for heat dissipation

and thermal runaway safety are some of the most critical problems requiring feasible solution before lithium-ion batteries is successfully commercialized for high power applications. Furthermore, an appropriate thermal management system is indeed required for optimal overall battery pack performance due to the fact that the temperature distribution within the battery cells and their electrochemical performance are strongly interdependent [3].

Jeon and Baek [4] employed the finite element analysis to investigate the transient heating process of a cylindrical lithium-ion battery cell during its discharge cycle. They found that joule heating contributes more significantly to the heating process at high discharge rates, but the entropy change dominates the heating process at low discharge rates. Later, Du et al. [5] analyzed the effect of discharge current on temperature variation using COMSOL MULTIPHYSICS. Very recently, Chen et al. [A6] have followed the trend and used the same software to study the dependence of thermal performance of a Panasonic 18650 lithium-ion battery cell on the rate of discharge current, the ambient temperature, the heat transfer coefficient on the cell surface, and electrode thickness.

The main goal for the thermal management system is to maintain high rate of heat dissipation from the lithium-ion battery cells so that they operate at an optimum temperature with small temperature variations within the modules and within the pack. To achieve these goals, conventional heat dissipation approaches such as forced air-cooling and liquid-cooling have been extensively developed for electric vehicle with additional installation of blowers, fans, pumps, pipes and other accessories [2].

The subject of current study is the second generation of the purely electric 8-seater car (as shown in Fig. 1) developed in the Department of Vehicle Engineering.

The specifications of its power system are listed in Table 1.

**Table 1. The specifications of the electric car shown in Fig. 1**

Rated power / speed:	24 kW/7200 rpm
Open circuit voltage:	96V
Battery voltage / quantity:	6V/16
Battery capacity:	216Ah
Maximum discharge rate:	0.5C

With the above electric current requirements, the configuration of a lithium-ion battery module can be designed. In this work, 18650 type lithium-ion battery cells were chosen to form the battery packs responsible for powering the purely electric car. The specifications of a commercial 18650 type lithium-ion cell have been summarized [7].



**Fig. 1. The electric car developed in the department**

In the processes of charging and discharging, lithium-ion battery cells generate a lot of heat leading to a rise in overall battery cell temperature. The uneven internal temperature of the cells causes the battery performance to become unstable and even serious impact on battery life and security. Therefore, the battery module cooling and its temperature control is critical to ensure the battery performance. The objective of current work is to simplify the heating model associated to a lithium-ion battery module that is applicable for the purely electric car shown in Fig. 1. The batteries are to be stored in the two white compartments under the first and second rows seats, as clearly seen in Fig. 1. The dimension of each compartment is 158 cm x 46 cm x 30 cm. The base of the compartment is made of 1-cm thickness wooden boards, the four vertical walls are made of aluminum plates, while the top wall consists of another piece of wooden board that is covered by a seat.

For the sake of lowering future computational burden, it is beneficial if the battery modules can be simplified and sufficiently represented by several rectangular heating boxes. With this simplified heat source, more detailed simulations, including the battery packs, the battery compartment, and its outside configurations, will become practical.

## II. METHODOLOGY

### 2.1. Electrothermal Properties of Battery Cell

According to the derivation of the battery heat equation by Bernardi et al. [8], the heat generation rate of a battery cell can be expressed as

$$\frac{dH_{total}}{dt} = \dot{q} - IE, \quad (1)$$

where  $dH_{total}/dt$  is the change in total enthalpy change over time,  $\dot{q}$  is the heat generation rate,  $I$  is the electric current, and  $E$  is the terminal voltage. By ignoring the effects of mixed enthalpy and phase change, the simplified electrochemical model used in this work reads

$$\dot{q} - IE = \sum_j I \left[ T^2 d \frac{U_{avg}}{dT} \right]. \quad (2)$$

Considering reversible chemical reaction, the heat generation rate of the lithium-ion battery can be expressed as

$$\dot{q} = I(E - U_{avg}) + IT \frac{\partial U_{avg}}{\partial T}. \quad (3)$$

The battery considered in this work is IHR18650 whose anode is made of lithium cobalt manganese nickel oxide. Under constant current discharge condition, the measurements of its open circuit voltage and battery terminal voltage have been reported by Du et al. [5]. The discharge current is between 1C to 5C, where 1C represents 2.5A. Hence, the maximum discharge current and the maximum voltage during discharge are 12.5A and 3.7V, respectively. Although lithium-ion battery cells generate heat when they are charged or discharged, they produce significantly more heat during discharge process. Therefore, this work only considers the situation when the battery cells are discharged. The electrochemical properties of the battery cell are integrated into heat generation scheme employed for each battery cell.

### 2.2. Governing Equations

Although the heat generated by all battery cells will trigger convective flows inside a battery module, the Reynolds number associated to the flow is very small. Therefore, it is reasonable to assume the flow of air trapped inside the battery module between two battery cells are laminar. Hence, the continuity, momentum, and energy equations for current study are given as followed [9]

$$\frac{\partial u}{\partial x} + \frac{\partial v}{\partial y} + \frac{\partial w}{\partial z} = 0, \quad (4)$$

$$\rho \left( \frac{\partial u}{\partial t} + u \frac{\partial u}{\partial x} + v \frac{\partial u}{\partial y} + w \frac{\partial u}{\partial z} \right) = - \frac{\partial p}{\partial x} + \mu \left( \frac{\partial^2 u}{\partial x^2} + \frac{\partial^2 u}{\partial y^2} + \frac{\partial^2 u}{\partial z^2} \right), \quad (5)$$

$$\rho \left( \frac{\partial v}{\partial t} + u \frac{\partial v}{\partial x} + v \frac{\partial v}{\partial y} + w \frac{\partial v}{\partial z} \right) = - \frac{\partial p}{\partial y} + \mu \left( \frac{\partial^2 v}{\partial x^2} + \frac{\partial^2 v}{\partial y^2} + \frac{\partial^2 v}{\partial z^2} \right), \quad (6)$$

$$\rho \left( \frac{\partial w}{\partial t} + u \frac{\partial w}{\partial x} + v \frac{\partial w}{\partial y} + w \frac{\partial w}{\partial z} \right) = - \frac{\partial p}{\partial z} + \rho g + \mu \left( \frac{\partial^2 w}{\partial x^2} + \frac{\partial^2 w}{\partial y^2} + \frac{\partial^2 w}{\partial z^2} \right), \quad (7)$$

$$\rho C_p \left( \frac{\partial T}{\partial t} + u \frac{\partial T}{\partial x} + v \frac{\partial T}{\partial y} + w \frac{\partial T}{\partial z} \right) =$$

$$+k \left( \frac{\partial^2 T}{\partial x^2} + \frac{\partial^2 T}{\partial y^2} + \frac{\partial^2 T}{\partial z^2} \right) + \dot{q}, \quad (8)$$

where the symbols appear in eqs. (4)-(8) follow conventional notation [9] while  $\dot{q}$  is given in eq. (3). To account for the thermal buoyancy, this work employed the Boussinesq approximation. For verification, the heating effect of a battery module consisting of 15 battery cells, as depicted in Fig. 2, was simulated. The green cylinders represent the battery cells while the gray box represents the aluminum battery module casing. For illustration, the lid to the case is not depicted in the figure.

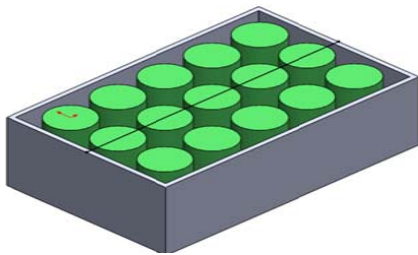


Fig. 2. The model used for verification

In addition to the 15-cell battery module mentioned above, two variations of 180-cell battery module designs were investigated. The design of these 7.2V/216Ah battery module geometry also took into consideration of the power requirement of the electric car as well as the structure of the battery compartment. The geometry of these battery modules is shown in Fig. 3.

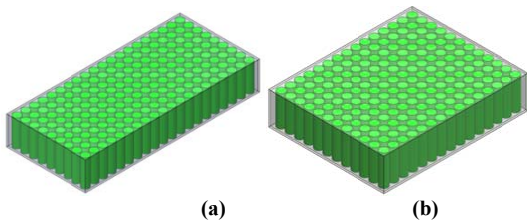


Fig. 3. The battery module considered in this work with different arrays: (a) 20 x 9; (b) 15 x 12

### III. RESULTS AND DISCUSSION

Although lithium-ion batteries do offer many advantages, operating the battery at the temperatures over its preferable range can cause damage to the battery cell itself. Generally, sophisticated electronic instruments are installed in the electric vehicles to control the charging and discharging process of each battery. However, controlling the temperature of the battery is a difficult task.

#### 3.1. Validation of Heating Parameters

In addition to the heat generation estimated using eq. (3), the aluminum casing for the battery module is assumed to be subjected to an external convective cooling corresponding to a heat transfer coefficient of  $20\text{W/m}^2\text{-K}$ . Figs. 4 compare the temperature distributions in the middle plane of the battery

module reported by Du et al. [5] and current simulation. These temperature distributions correspond to a discharge current of 5C for different depths of discharge (DOD). DOD is a measurement of how deeply the battery is discharged. Fig. 5 displays the temperature profiles along the line shown in Fig. 2 when SOC = 5. These figures have clearly proven that current study is capable of producing very similar results published in the literature. However, the temperature readings close to the casing show greater discrepancy. This is because the casing material is not explicitly documented in the literature.

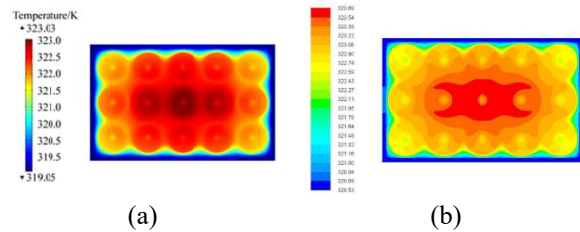


Fig. 4. Comparison of result: (a) Du et al. [5]; (b) current

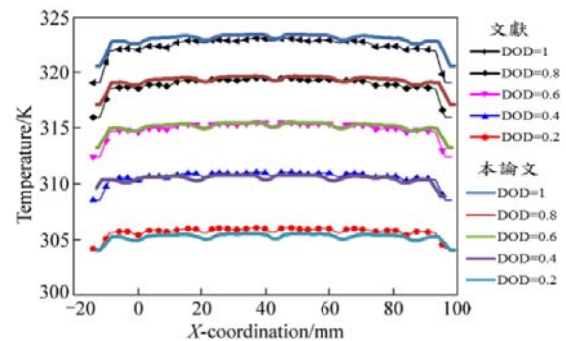
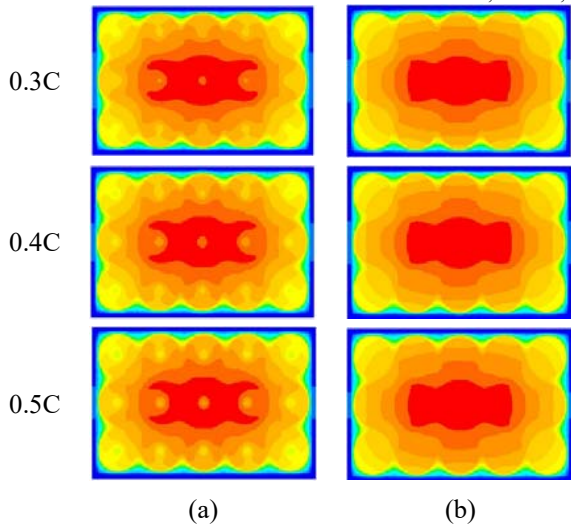


Fig. 5. Temperature profiles at different DOD's

#### 3.2. Homogeneous Heating of Battery Cell

In actual situations, heat dissipation only occurs through the battery walls other than its core. Capturing this behavior requires more demanding meshing scheme as well as greater sophistication when dealing with thermal boundary condition. To simplify current simulation, it is more desirable to assume that the entire battery including its 4mm-diameter core also generates heat at a rate identical to rest of the battery cell. Figs. 6 show the temperature distributions presented in the literature [5] in comparison with current results if the battery cell is treated as a cylinder with constant rate of heat generation. It is found that the temperature distributions are generally quite similar with each other. This proves the feasibility of representing each battery cell with a cylinder. Apparently, the regions of lower temperature at the center of each battery cell are absent if the cores of the battery cells are assumed to be generating heat.

To further examine the feasibility of treating the battery cell as a uniform heat generating cylinder, this work compares the average surface temperature of the battery corresponding to different discharge



**Fig. 6. Temperature variation at different discharge currents: (a) non-heating battery core, and (b) heating battery core**

currents. As shown in Fig. 7, the simplified model yields identical average surface temperature. This clearly proves that despite the absence of the lower temperature region on top of each battery cell, the difference in temperature readings on each battery cell is negligible.

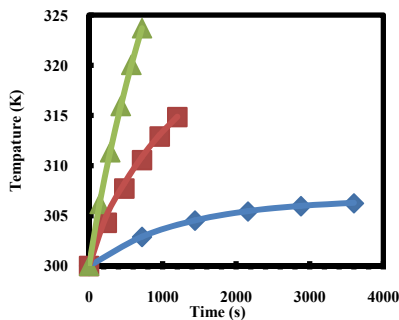


**Fig. 7. Comparison of average temperature of battery surface for different discharge currents: (a) symbol - non-heating battery core, and (b) line - heating battery**

Figs. 8 show the temperature distribution on the lid of the battery module casing. It is important to emphasize that the maximum temperature difference between the red and dark blue regions are less than 1°C for 0.3C and 0.4C and slightly greater than 1°C for 0.5C. Not only so, it is found that the presence of the spacing between two neighboring battery cells cannot be identified solely through the temperature distribution. This somewhat postulates that the aluminum battery module casing is very effective in dissipating heat along with heat conduction. On the other hand, the 20x9 array has slightly over-performed the 15x20 array for the former array has slightly higher temperature distribution and narrower range of temperature. Regardless of the insignificant difference in heat dissipation effectiveness, it can be deduced that the decision about which array to be

used in the electric car should be focus on the convective heat effect outside of the battery modules. Furthermore, the heating process of the 20x9 and 15x12 battery arrays were investigated. Their surface temperatures were averaged and presented in Fig. 9. As seen in the figure, the surface temperature increases with the amount of discharge current. In the beginning of the discharge process, the temperature of the battery modules increases sharply until a point in time when its rise begins to slow down. This proves that there exists a steady-state condition where the amount of heat generated in the battery cells balances with the amount of heat removed by the battery module casing. Although the two battery arrays show similar trends, the battery module casing with 20x9 array is actually slightly warmer than the one with 15x12 array.

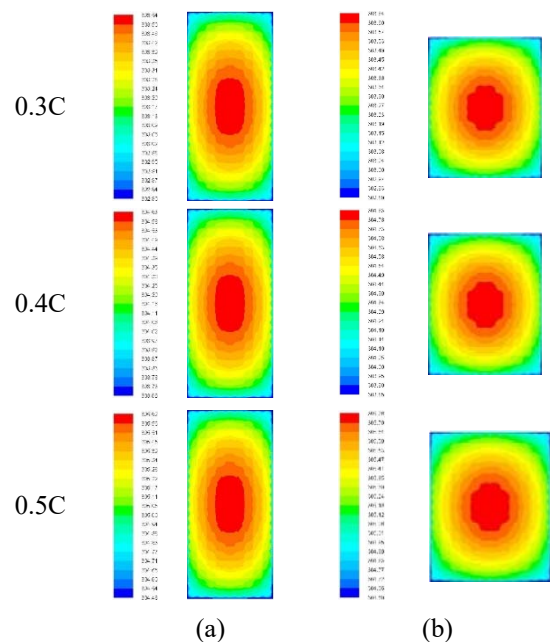


**Fig. 8. Temperature variation with different arrays: (a) 20x9; (b) 15x12**

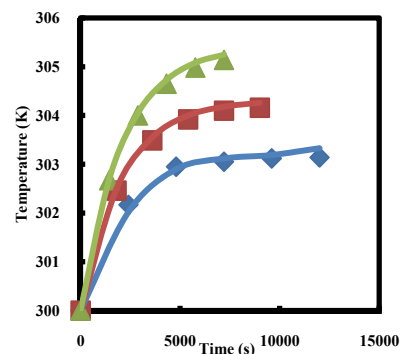


**Fig. 9. Comparison of average surface temperature on the battery module for different discharge currents: (a) symbol - 20 x 9 array, and (b) line - 15 x 12 array**

In order to visualize the uniformity of the surface temperature on the battery module, the values of the



surface temperature were statistically analyzed. The average surface temperature, its variance, and standard deviation were calculated. Based on the average and variance, the scattering of these temperature values is presented in Fig. 10 using normal distribution. As the battery cells discharge, the surface of the cell module tends to heat up. As seen in the figure, at 0.3C, the average temperature gradually increases from roughly 302.3°C at 1440s (24 min) to roughly 303.3°C at 5760s (96 min). Also notice is that the range of temperature increases with the duration of battery discharge. On the other hand, the probability density decrease. This indicates that everywhere on the battery module surface heats up,

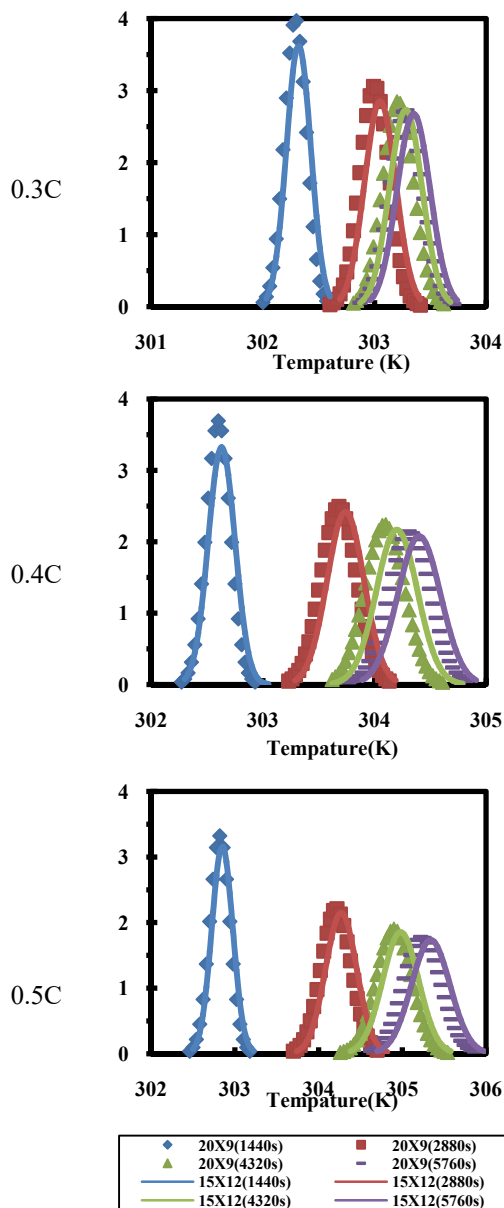


Fig. 10. Temperature variation at different discharge currents: (a) non-heating battery core, and (b) heating battery but the difference between its maximum and minimum temperature readings become greater.

From these figures, one also find that both the battery module of 20x9 and 15x12 arrays are quite similar in terms of temperature variation. However, the 20x9 array does yields the lower temperature, in a strict sense. The rate of temperature increases with the discharge current. For an example, the average battery module surface temperature associated to 0.3C is less than 304°C at 1440s while that associated to 0.5C is more than 305°C.

### 3.3. Homogeneous Heating of Battery Cell

It is the objective of current study to further simplify the battery module by employing lumped-system approach. Instead of modeling each battery cell contained in the casing, the lumped-system approach treats the entire battery module as a single solid unit that generates volumetric heat at the rate.

As shown in Fig. 11, the temperature distribution for the lumped system model is smoother than the separated battery model. The lumped-system approach yields higher surface temperatures on the casing. However, it is remarkable to point out that the temperature differences shown in Fig. 11(a) and (b) are very small.

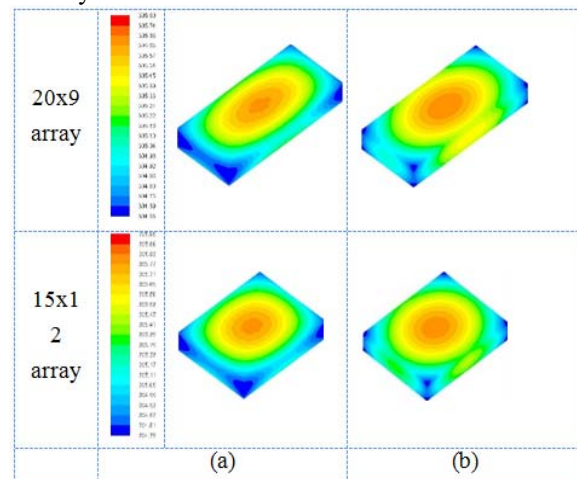


Fig. 11. Temperature distributions on the casing: (a) separated battery model; (b) lumped system model;

The progress of the average surface temperature over time on the casing for both models are presented in Figs. 12. Clearly, the lumped-system approach generally yields higher average temperature in comparison with that obtained using the separated battery approach. However, the discrepancy between the two approaches is evidently very small in the condition that the rate of heat generation is correctly applied throughout the entire domain. In this work, this value is assigned 3 kW/m<sup>3</sup> for 0.3C, 4 kW/m<sup>3</sup> for 0.4C, and 5 kW/m<sup>3</sup> for 0.5C. Although these values of rate of heat generation was not optimized to yield the best comparison between the separated battery model and the lumped system model, the relationship between the rate of heat generation assigned and the discharge current has obviously demonstrated a linear correlation even if it may not be perfectly linear.

In addition to the average surface temperature presented in Fig. 12, the overall heat fluxes across the casing are plotted in Fig. 13. Unlike the average temperature, heat flux seems to demonstrate more comparable values between the separated battery model and the lumped system model. Consistent with intuition, the higher the discharge current, the greater the battery module produces heat and hence in greater need for effective heat removal strategy.

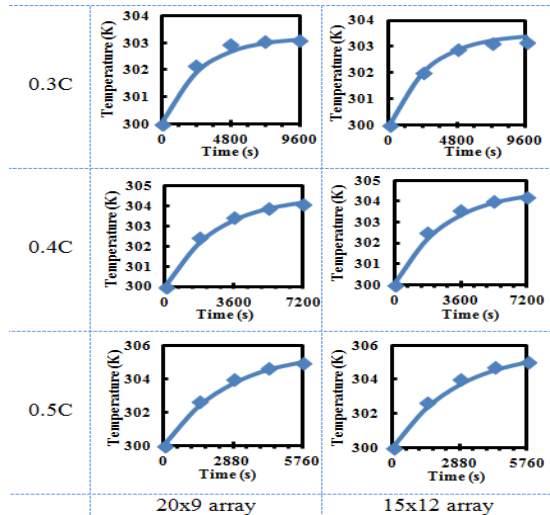


Fig. 12. Average surface temperatures: (a) line - separated battery model; (b) symbol - lumped system model

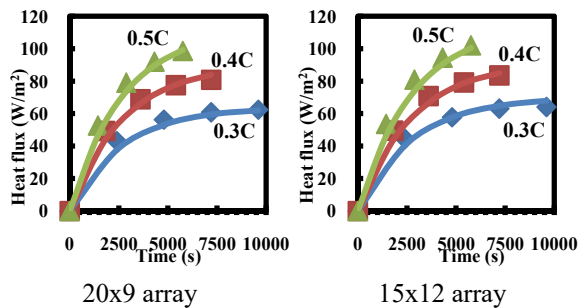


Fig. 13. Temperature distributions on the casing: (a) line - separated battery model; (b) symbol - lumped system model

## CONCLUSIONS

This work proposes two lithium-ion battery module arrays for a target electric car and investigates their heating phenomenon when the battery cells are discharged. Their appropriate cooling schemes when

stored in the battery compartment will be studied. The major conclusions are as follows:

1. The lumped-system approach can be applied to simplify the more complicated approach where each battery cell is modeled.
2. The 20x9 battery cell array yields lower average temperature on the module surface.
3. After discharge, the temperature rise for the individual battery in the 15x12 battery module is relatively uneven. At a discharge rate of 0.5C, the greatest difference of the individual battery surface temperature in the battery module is 1.16°C.

## ACKNOWLEDGMENTS

The financial support by the Ministry of Science and Technology through MOST 107-2637-E-020-004 is greatly appreciated.

## REFERENCES

- [1] S. Al-Hallaj, H. Maleki, J.S. Hong, and J.R. Selman, "Thermal modeling and design considerations of lithium-ion batteries," *Journal of Power Source*, vol. 83, pp.1–8, 1999.
- [2] A.A. Pesaran, A. Vlahinos, and S.D. Burch, "Thermal performance of EV and HEV battery modules and pack," *Proceeding of the 14th International Symposium, Orlando, FL, Dec. 15-17, 1997*.
- [3] M.-S. Wu, K.H. Liu, Y.-Y. Wang and C.-C. Wan, "Heat dissipation design for lithium-ion batteries," *Journal of Power Source*, vol. 109, pp.160–166, 2002.
- [4] D.H. Jeon, and S.M. Baek, "Thermal modeling of cylindrical lithium ion battery during discharge cycle," *Energy Conversion and Management*, vol. 52, pp.2973–2981, 2011.
- [5] S.-L. Du, Y.-Q. Lai, M. Jia, Y. Cheng, H.-L. Zhang, K. Zhang, and Y.-X. Liu, "Electrothermal characteristics simulation of cylindrical automotive lithium-ion battery," *The Chinese Journal of Nonferrous Metals*, vol. 24, pp.1823–1830, 2014.
- [6] J. Chen, H. Kang, and Z. Tan, "Analysis of thermal performance of 18650 li-ion battery based on an electrochemical-thermal coupling model," *Hans Journal of Chemical Engineering and Technology*, vol. 8(2), pp.97–107, 2018.
- [7] S.A. Khateeb, M.M. Farid, J.R. Selman, and S. Al-Hallaj, "Design and simulation of a lithium-ion battery with a phase change material thermal management system for an electric scooter," *Journal of Power Sources*, vol. 128, pp. 292–307, 2004.
- [8] D. Bernardi, E. Pawlikowski, and J. Newman, "A general energy balance for battery systems," *Journal of The Electrochemical Society*, vol. 132(1), pp. 5–12, 1985.
- [9] M. Favre-Marinet, and S. Tardu, *Convective Heat Transfer*, John Wiley & Sons, Inc., New Jersey, USA, 2009.

★ ★ ★